

# Self-trapped Exciton and Franck-Condon Spectra Predicted in LaMnO<sub>3</sub>

Philip B. Allen and Vasili Perebeinos

Department of Physics and Astronomy, State University of New York, Stony Brook, New York 11794-3800  
(August 6, 2018)

Because the ground state has cooperative Jahn-Teller order, electronic excitations in LaMnO<sub>3</sub> are predicted to self-trap by local rearrangement of the lattice. The optical spectrum should show a Franck-Condon series, that is, a Gaussian envelope of vibrational sidebands. Existing data are reinterpreted in this way. The Raman spectrum is predicted to have strong multiphonon features.

71.35.Aa,71.38.+i,78.20.Bh,75.30.Vn

In small molecules, excited electronic states generally have altered atomic coordinates, which leads to Franck-Condon multi-phonon sidebands in electronic spectra [1]. In solids, electronic excited states are often delocalized, eliminating such effects [2]. However, if excited states self-localize [3,4] then Franck-Condon effects should reappear in the form of Gaussian broadening of the pure electronic transition [5]. Here we argue that such effects are crucial to a correct interpretation of LaMnO<sub>3</sub>, the parent compound of the “colossal magnetoresistance” materials.

LaMnO<sub>3</sub> has a cubic to orthorhombic cooperative JT distortion [6] at 800K which corresponds to wavevector  $\vec{Q} = (\pi, \pi, 0)$ . This drives orbital order [7]:  $x$  and  $y$ -oriented  $e_g$  orbitals alternate in the  $x - y$  plane, in a layer structure shown schematically in Fig. 1. A “minimal” model has two Mn  $d$  orbitals ( $e_g$  states  $\psi_{x^2-y^2}$  and  $\psi_{3z^2-r^2}$ ), Hubbard  $U$ , Hund energy  $J$  to align the  $e_g$  spin with the  $S = 3/2$  spin of the  $3 t_{2g}$  electrons, a hopping term permitting band formation, and very important, electron-phonon coupling which allows local distortions of the oxygen environment to split the energies of the singly occupied  $e_g$  levels and drive the JT transition.

The highly-doped phases of LaMnO<sub>3</sub> show a remarkable interplay of charge, orbital, and spin order [8]. The relative importance of Coulomb, electron-phonon, and other effects is controversial. For light doping, however, charge order is not an issue and the problem simplifies. With no “empty” (Mn<sup>4+</sup>) sites for an  $e_g$  electron to hop into, the large size of  $U$  suppresses hopping. The electron-phonon term becomes the dominant part of the remaining Hamiltonian, and is simple enough that low-temperature properties can be solved. We have already reported [9] properties of the self-trapped hole (“anti Jahn-Teller” small polaron) which forms at low doping. Its sensitivity to spin order influences the magnetic states seen at low doping. We also gave a preliminary treatment of electronic excitations [10]. Here we give a more complete solution for the lowest electronic excitation, finding a self-trapped exciton, insensitive to spin order, whose Franck-Condon effect should dominate  $\sigma(\omega)$  and the resonant Raman spectrum, and might also appear in luminescence. These results follow cleanly from our model, but have not previously been recognized as relevant.

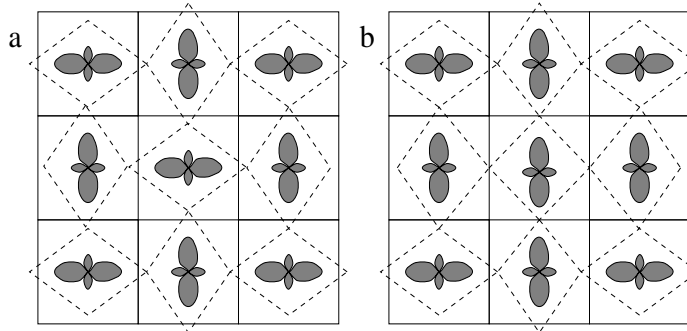


FIG. 1. a. schematic of Jahn-Teller distorted LaMnO<sub>3</sub>  $x - y$  plane with orbitals ordered. b. The lowest electronic excitation with an orbital rotated and the lattice relaxed.

We make the strong-coupling approximation  $U \rightarrow \infty$  by considering only states with no double occupancy of  $e_g$  orbitals; this suppresses hopping and leaves only two terms in the Hamiltonian. Vibrational degrees of freedom are modelled by allowing each oxygen to move along the nearest-neighbor Mn-O-Mn axis,

$$\mathcal{H}_{\text{vib}} = \sum_{\ell,\alpha=x,y,z} (P_{\ell,\alpha}^2/2M + Ku_{\ell,\alpha}^2/2). \quad (1)$$

Here  $u_{\ell,x}$  is the displacement from cubic perovskite position of the nearest oxygen in the  $x$ -direction to the Mn atom at  $\ell$ . The Jahn-Teller energy is modelled by a linear reduction of energy of an occupied  $3x^2 - r^2$  orbital if the

corresponding two oxygens in the  $\pm\hat{x}$  direction expand outwards, and similarly for  $\hat{y}$  and  $\hat{z}$  oxygens if  $3y^2 - r^2$  or  $3z^2 - r^2$  orbitals are occupied,

$$\mathcal{H}_{\text{JT}} = -g \sum_{\ell,\alpha} \hat{n}_{\ell,\alpha} (u_{\ell,\alpha} - u_{\ell,-\alpha}). \quad (2)$$

Here  $\hat{n}_{\ell,x}$  is the occupation number of the  $3x^2 - r^2$  orbital, and  $u_{\ell,-x}$  is the displacement of the oxygen nearest the Mn atom at  $\ell$  in the  $-x$ -direction. Since no hopping occurs in this model, the type and degree of magnetic order is irrelevant, and no change occurs in the electronic spectrum as  $T$  is increased through the Neel temperature  $T_N = 140\text{K}$ .

The adiabatic parameter is  $\alpha = \hbar\omega_0/\Delta$  where  $\omega_0 = \sqrt{K/M} \approx 75\text{ meV}$  is the oxygen vibration frequency [11] and  $2\Delta \approx 1.9\text{ eV}$  is the Jahn-Teller gap (explained below.) Since  $\alpha$  is small, we solve the Hamiltonian in adiabatic approximation, then add quantized lattice vibrations. There is an infinite set of equally good distorted ground states [12] whose degeneracy is broken by anharmonic terms left out of the minimal  $\mathcal{H} = \mathcal{H}_{\text{vib}} + \mathcal{H}_{\text{JT}}$ . We simply adopt the distortion seen experimentally and shown in Fig. 1. The A sublattice is defined to be Mn sites where  $\exp(i\vec{Q} \cdot \vec{\ell})$  is 1, and the B sublattice to be sites where it is -1. The resulting ground state electronic wavefunction [9] is

$$|0\rangle = \prod_{\ell}^A c_X^\dagger(\ell) \prod_{\ell'}^B c_Y^\dagger(\ell') |\{0\}\rangle, \quad (3)$$

where  $|\{0\}\rangle$  refers to the lattice state with oxygens displaced by  $\pm u_0 = 2g/K$  as shown in Fig. 1 and in their vibrational ground states. The orbitals  $\psi_X$  and  $\psi_Y$  which are occupied on the A and B sublattices are orthogonal  $x$ - and  $y$ -directed states  $\psi_{X,Y} = (-\psi_{3z^2-r^2} \pm \psi_{x^2-y^2})/\sqrt{2}$ . In state (3) each occupied Mn orbital has its energy lowered by  $\Delta = 8g^2/K$  and each unoccupied orbital has its energy raised by  $\Delta$ . This costs elastic energy  $Ku_0^2 = \Delta/2$  per Mn atom (two of the three oxygen atoms per Mn site are displaced) giving a total condensation energy of  $-\Delta/2$  per Mn. Our picture is substantially the same as the earlier theory by Millis [12].

If oxygen atoms were frozen in these optimal positions, the lowest electronic excitation (an “orbital defect,” Fig. 1 b) would cost  $2\Delta = 1.9\text{ eV}$ , the JT gap. This would form a narrow “orbiton” band [10] because terms of order  $t^2/U$  (neglected here) allow the orbital defect to exchange sites, lowering the energy by  $t^2/U$ . However, there is a much greater energy lowering if instead the lattice locally **undistorts**, pinning the orbital excitation on a single site as shown in Fig. 1b. This reduces the energy of the orbital defect from  $2\Delta$  to  $\Delta$ . Thus the lowest electronic excitation is a strongly self-trapped exciton, somewhat like the Frenkel exciton seen in molecular crystals [2].

If this excitation is excited optically, the Franck-Condon principle applies, and a sequence of vibrational sidebands of the localized exciton will appear in the spectrum. The optical conductivity is

$$\sigma(\omega) = \frac{\pi Ne^2\omega}{\Omega} \sum_{n,n'} \frac{e^{-\beta n_i \hbar\omega_0}}{Z} | \langle fn' | \hat{\epsilon} \cdot \vec{r} | in \rangle |^2 \delta(\Delta + (n_f - n_i)\hbar\omega_0 - \hbar\omega), \quad (4)$$

where  $\Omega$  is the volume of the crystal, and the number of cells  $N$  appears because the localized excitation can be created on any Mn atom. The partition function  $Z$  is  $(1 - \exp(\beta\hbar\omega_0))^{-6}$  because 6 oscillators couple to each electronic transition. The required dipole matrix element is

$$\langle fn' | \hat{\epsilon} \cdot \vec{r} | in \rangle = \int d^6R \int d\vec{r} \chi_{n'}(R - R_f) \psi_Y(\vec{r}, R) \hat{\epsilon}_L \cdot \vec{r} \psi_X(\vec{r}, R) \chi_n(R - R_i). \quad (5)$$

The crystal starts in state  $|in\rangle$  with an electron at site 0 in the electronic ground state  $|i\rangle = |X\rangle$  with equilibrium coordinates  $R_i$  and vibrational quanta of the 6 surrounding oxygens denoted by  $\{n\} = (n_1, n_2, n_3, n_4, n_5, n_6)$ . It ends up at the same site in final state  $|fn'\rangle$  with the electron in state  $|f\rangle = |Y\rangle$  of energy  $\Delta$  with new equilibrium positions  $R_f$  and new vibrational quanta  $\{n'\} = (n'_1, n'_2, n'_3, n'_4, n'_5, n'_6)$ . The notation  $n_i$  denotes the total initial vibrational level  $n_1 + \dots + n_6$ , and  $n_f$  is the total final vibrational level. The electronic part of the matrix element is a  $d$  to  $d$  transition which is forbidden when the surroundings are symmetric (as in the starting coordinates  $R_i$  or the final coordinates  $R_f$  if  $n_i = n_f = 0$ ). The origin of the observed optical transitions has been discussed by various authors [13–15]. In our localized picture with lattice displacements as primary factors, it is natural to recognize that any asymmetric oxygen breathing displacement will cause the Mn  $e_g$  orbitals to acquire an admixture of  $4p$  character. A typical mixing coefficient is

$$\gamma = \int d\vec{r} \psi_{3z^2-r^2} \frac{\partial V}{\partial u_5} \psi_z / (\epsilon_d - \epsilon_p) \quad (6)$$

where  $\psi_z$  is an orbital of  $p$ -character, partly Mn  $4p$ , and partly oxygen  $2p$ ;  $\partial V/\partial u_5$  is the perturbation caused by a displacement of oxygen 5 in the  $\hat{z}$ -direction. The corresponding allowed optical matrix element is

$$d = \int d\vec{r} \psi_{3z^2-r^2} z \psi_z. \quad (7)$$

The resulting matrix element, Eqn. 5, is

$$\langle fn'|\hat{\epsilon} \cdot \vec{r}|in \rangle = \frac{\gamma d}{2} \langle n'_1 n'_2 n'_3 n'_4 n'_5 n'_6 | [(u_1 + u_2)\epsilon_x + (u_3 + u_4)\epsilon_y - 2(u_5 + u_6)\epsilon_z] | n_1 n_2 n_3 n_4 n_5 n_6 \rangle \quad (8)$$

The general term (8) is complicated; we have evaluated only when the initial state has  $n_i = 0$  or 1 quanta of vibration. Two or more quanta occur at <6% probability at 300K. Our approximate optical conductivity is then

$$\sigma(\omega) = \frac{1}{Z} [\sigma_0(\omega) + e^{-\beta\hbar\omega_0} \sigma_1(\omega) + \dots] \quad (9)$$

The vibrational overlap integrals needed for  $\sigma_0$  are

$$\langle n_1 | 0 \rangle = \left( \frac{M\omega_0}{2\hbar} \right)^{n_1/2} \frac{(-u_0)^{n_1}}{\sqrt{n_1!}} \exp \left( -\frac{M\omega_0 u_0^2}{4\hbar} \right) \quad (10)$$

$$\langle n_1 | u_1 | 0 \rangle = \left( \frac{u_0}{2} - \frac{n_1 \hbar}{M\omega_0 u_0} \right) \langle n_1 | 0 \rangle. \quad (11)$$

and similar for states 2,3,4 except that for states 2 and 4,  $-u_0$  is replaced by  $+u_0$ ; this changes the sign of the prefactor of Eqn. 11. We find that for both  $\sigma_0$  and  $\sigma_1$ ,  $\sigma_{xx} = \sigma_{yy} = \sigma_{zz}/4$ . The answer for  $\sigma_0$  is

$$\sigma_{0,zz}(\omega) = (\gamma d)^2 \frac{\pi e^2}{M} \frac{N}{\Omega} \frac{\omega}{\omega_0} \sum_{n=0}^{\infty} \frac{(\Delta/\hbar\omega_0)^n}{n!} \exp \left( -\frac{\Delta}{\hbar\omega_0} \right) \delta \left( \frac{\Delta}{\hbar} + (n+1)\omega_0 - \omega \right). \quad (12)$$

The formula for  $\sigma_1$  is more complicated and will not be given here.

Our theory compares reasonably well with experiment.  $\sigma(\omega)$  has been measured by reflectivity on polycrystalline samples at room temperature [13,16], single crystals at low  $T$  [17], and cleaved single crystals at room temperature [18], all with consistent results. Jung *et al.* [16] have expressed their  $\sigma(\omega)$  as a sum of Lorentzian peaks. The lowest peak is centered around 1.9 eV with a width of 1 eV. Fig. 2 shows their Lorentzian fit, and compares with our theory, with  $2\Delta = 1.9$  eV and amplitude chosen to agree with experiment.

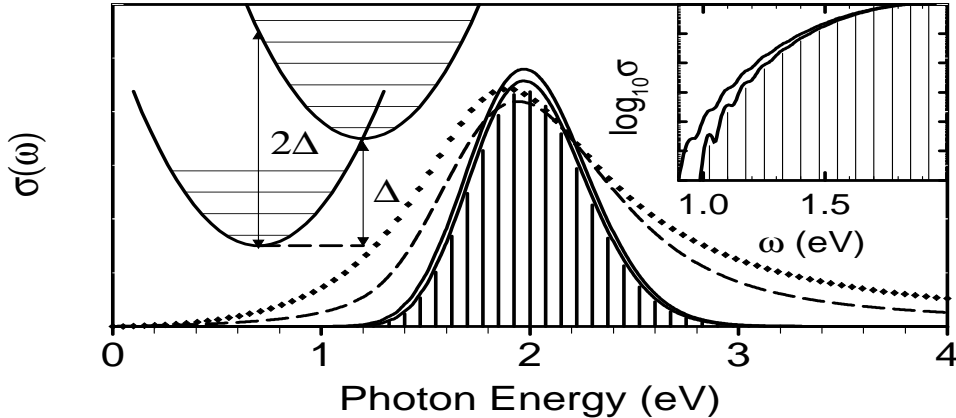


FIG. 2. Optical conductivity of  $\text{LaMnO}_3$ . The points are the lowest Lorentzian oscillator fit by Jung *et al.* to their data. The dashed curve is a  $T = 0$  sum of convolved Lorentzians centered at the vibrational replicas shown as vertical bars; the solid curves are  $T = 0$  (lower) and  $T = 300\text{K}$  (upper) sums of convolved Gaussians, also shown in the inset on a logarithmic scale. Tick marks in the inset denote decades.

The intensity seen experimentally [16] corresponds to  $f=0.16$  oscillators per Mn atom in the lowest peak, where  $\int d\omega\sigma(\omega)$  is defined as  $(\pi Ne^2/2m\Omega)f$ , with  $m$  the electron mass. Our theory gives  $f = 2(\gamma d)^2(m/M)(2\Delta/\hbar\omega_0 + 1)$  and has the value  $0.18(\gamma d)^2 \times 10^{-2}$ . To agree with experiment,  $\gamma d$  must be 10. This is reasonable since the electron-phonon mixing coefficient may be a few per Å oxygen displacement, while the dipole matrix element is likely to be a few Å. Most authors [13–17] agree in assigning the 2 eV structure to  $e_g$  to  $e_g$  transitions activated by mixing of  $p$ -character, usually from surrounding oxygens. However, the origin of the mixing is usually taken as the dispersive broadening of the  $e_g$  bands; in our strong-coupling picture, these effects enter at order  $t/U$  and are neglected, but might be comparable to the phonon effects which we calculate explicitly.

The delta function peaks of our model theory should be replaced by local densities of vibrational states on oxygen atoms. If this is mimicked by using a sequence of convolved Lorentzians ( $L, L * L, \dots$ ) the result agrees closely with experiment. A sequence of convolved Gaussians may be more realistic, and is shown in Fig. 2 as a dashed line and enlarged on a logarithmic scale. Our theory is not the only candidate; band theory [19] yields reasonable agreement at  $T = 0$ . However, our theory makes definite predictions which differ from those of band theory. We find the onset of absorption at  $T = 0$  to be the one-phonon structure at  $\Delta + \omega_{\text{ph}} \approx 1$  eV, weaker by  $10^4$  than the  $2\Delta=1.9$  eV peak absorption. The fine structure of subsequent phonon peaks will be harder to resolve because of increasing multiplicity of vibrational quanta available for multi-phonon absorption. Another definite prediction concerns temperature dependence. Contrary to approaches using dispersive bands [19,15],  $\sigma(\omega)$  in our approach is not affected by the loss of magnetic order as temperature increases. Contrary to band theory, we predict very weak temperature effects near the absorption peak at  $2\Delta$ , consistent with experiment [17,18]. By contrast we predict big changes of intensity in the weak features near  $\omega = \Delta$ , including new weak peaks at  $\Delta - n\omega_{\text{ph}}$  for  $n = 0, 1, \dots$  activated by temperature, and shown in the inset to Fig. 2. These effects are too small to be seen in existing reflectivity data, but should be measurable by absorption in very clean thin films. If electronic excitations survive long enough to relax by luminescence, then a very large Stokes shift is predicted.

Another manifestation of the Franck-Condon effect should appear in the Raman spectrum [20], particularly if the laser frequency is near the  $2\Delta=1.9$  eV Jahn-Teller gap edge. Multi-phonon Raman features should appear with intensity similar to the one-phonon spectrum. The incident photon creates (among various other virtual excitations) a self-trapped exciton in a superposition of multi-phonon states (as in the left inset of Fig. 2.) The virtual exciton can reemit a photon, returning either to the ground state or (with nearly equal amplitude) to various one-phonon or multi-phonon excited states. The theory was given by Shorygin [21]. A particularly clear solid-state example is Martin's [22] observation of multiples of the localized phonons of the  $\text{MnO}_4^{2-}$  impurity complex in CsI. Multiples of the Jahn-Teller related vibrations should appear in the Raman spectrum of  $\text{LaMnO}_3$ , but less distinct than in Martin's work since the local phonon density of Jahn-Teller vibrations will be less localized and correspondingly less well-structured. Published Raman measurements [11] on undoped  $\text{LaMnO}_3$  do not extend to the multi-phonon region. An unpublished two-phonon replica of the Jahn-Teller phonon in  $\text{LaSr}_2\text{Mn}_2\text{O}_7$  is seen by Romero *et al.* [23], and similar features are seen in unpublished [24] work on  $\text{LaMnO}_3$ . These are probably the effect we are predicting.

## ACKNOWLEDGMENTS

We thank M. Blume, M. Cardona, J. P. Hill, T. P. Martin, L. Mihaly, A. J. Millis, and D. Romero for help. This work was supported in part by NSF grant no. DMR-9725037.

---

- [1] G. Herzberg, *Spectra of Diatomic Molecules*, 2nd Ed., Van Nostrand, New York, 1950.
- [2] *Excitons*, edited by E. I. Rashba and M. D. Sturge (North-Holland, Amsterdam, 1982).
- [3] E. I. Rashba, in ref. 2, pp. 543-602.
- [4] K. S. Song and R. T. Williams, *Self-Trapped Excitons*, Springer, Berlin, 1993.
- [5] K. Cho and Y. Toyozawa, *J. Phys. Soc. Jpn.* **30**, 1555 (1971); H. Sumi, *J. Phys. Soc. Jpn.* **38**, 825 (1975).
- [6] J. Rodriguez-Carvajal, M. Hennion, F. Moussa, A. H. Moudden, L. Pinsard, and A. Revcolevschi, *Phys. Rev. B* **57**, 3189 (1998).
- [7] Y. Murakami, J. P. Hill, D. Gibbs, M. Blume, I. Koyama, M. Tanaka, H. Kawata, T. Arima, Y. Tokura, K. Hirota, and Y. Endoh, *Phys. Rev. Lett.* **81**, 582 (1998).
- [8] C. N. R. Rao and B. Raveau, editors, *Colossal Magnetoresistance, Charge Ordering, and Related Properties of Manganese Oxides*, (World Scientific, Singapore, 1998).

- [9] P. B. Allen and V. Perebeinos, Phys. Rev. B **60**, xxxx (1999).
- [10] V. Perebeinos and P. B. Allen, Phys. Stat. Sol. (b) **215**, 607 (1999).
- [11] M. N. Iliev, M. V. Abrashev, H.-G. Lee, V. N. Popov, Y. Y. Sun, C. Thomsen, R. L. Meng, and C. W. Chu, Phys. Rev. B **57**, 2872 (1998); V. B. Podobedov, A. Weber, D. Romero, J. P. Rice and H. D. Drew, Phys. Rev. B **58**, 43 (1998); E. Granado, N. O. Moreno, A. Garcia, J. A. Sanjurjo, C. Rettory, I. Torriani, S. B. Oseroff, J. J. Neumeier, K. J. McClellan, S.-W. Cheong, and Y. Tokura, Phys. Rev. B **58**, 11435 (1998); C. Roy and R. C. Budhani, J. Appl. Phys. **85**, 3124 (1999); A. de Andrés, J. L. Martínez, J. M. Alonso, E. Herrero, C. Prieto, J. A. Alonso, F. Agulló, and M. García-Hernández, J. Magn. Magn. Mat. **196-197**, 453 (1999).
- [12] A. J. Millis, Phys. Rev. B **53**, 8434 (1996).
- [13] T. Arima, Y. Tokura, and J. B. Torrance, Phys. Rev. B **48**, 17006 (1993).
- [14] I. S. Elfimov, V. I. Anisimov, and G. A. Sawatzky, Phys. Rev. Letters **82**, 4264 (1999).
- [15] K. H. Ahn and A. J. Millis, cond-mat/9901127.
- [16] J. H. Jung, K. H. Kim, D. J. Eom, T. W. Noh, E. J. Choi, J. Yu, Y. S. Kwon, and Y. Chung, Phys. Rev. B **55**, 15489 (1997); J. H. Jung, K. H. Kim, T. W. Noh, E. J. Choi, and J. Yu, Phys. Rev. B **57**, 11043 (1998).
- [17] Y. Okimoto, T. Katsufuji, T. Ishikawa, T. Arima, and Y. Tokura, Phys. Rev. B **55**, 4206 (1997).
- [18] K. Takenaka, K. Iida, Y. Sawaki, S. Sugai, Y. Moritomo, and A. Nakamura, cond-mat/9810035.
- [19] I. Solovyev, N. Hamada, and K. Terakura, Phys. Rev. B **53**, 7158 (1996).
- [20] G. Güntherodt and R. Merlin, in *Light Scattering in Solids IV*, edited by M. Cardona and G. Güntherodt (Springer Verlag, Berlin, 1984), p.256 ff.
- [21] P. P. Shorygin, Sov. Phys. – Usp. **16**, 99 (1973).
- [22] T. P. Martin and S. Onari, Phys. Rev. B **15**, 1093 (1977).
- [23] D. B. Romero, V. B. Podobedov, A. Weber, J. F. Mitchell, Y. Moritomo, and H. D. Drew, preprint.
- [24] D. B. Romero, private communication.